

# Buckling Analysis of Composite Plates Under Thermo-Mechanical Loading

**Prof. Dr. Adnan N.Jameel**

**Hasanain I. Nsaif**

University of Baghdad

College of Engineering

Mechanical Engineering Department

**Abstract:** *Buckling analysis of composite laminates for critical thermal (uniform and linear) and thermo-mechanical loads is reported here. The objective of this work is to carry out a theoretical investigation of composite plates under thermo-mechanical loads. The analytical investigation involved certain mathematical preliminaries, a study of equations of orthotropic elasticity for classical laminated plate theory (CLPT), higher order shear deformation plate theory (HSDT), and numerical analysis (Finite element method), then the equation of motion are derived and solved using Navier method and Levy method for symmetric and anti-symmetric cross-ply and angle-ply laminated plates to obtain buckling load by solving eigenvalue problem for different boundary conditions under different thermo-*

*mechanical loading. The work also contained a verification study of these methods with those published by other researchers. The results obtained gives good agreement. The experimental investigation is to find mechanical properties at room temperature of glass-polyester. Analytical and numerical results of critical buckling load studied the effect of boundary conditions, No. of layers, No. of half wavelengths, lamination angle, aspect ratio ,and thickness ratio on buckling load under different thermo-mechanical loading condition.*

## **1. Introduction**

Fiber-reinforced composites are used extensively in the form of relatively plate, and consequently the load carrying capability of composite plate against buckling have been intensively considered by researchers under various loading and boundary conditions. The initial theoretical research into buckling analysis was Gossard et al. 1952[1] outlined an approximate method (Ritz method) based on von Karman large-deflection plate theory for calculating the deflections of flat plates subjects to thermal buckling theoretically and experimentally. This method is used to determine the deflections of a simply supported plate subjected to a temperature distribution over the plate surface. Thangaratnam K. R. et al. 1988[2] studied buckling analysis of composite laminates for critical temperature under thermal load based on finite element method using semiloof element. Prabhu M.R. and Dhanaraj R. 1994[3] analyzed thermal buckling of laminated composite plate using finite element method. Nine node elements are employed for thermal buckling analysis of symmetric cross-ply and angle-ply

laminates subjected to uniform temperature distribution. The effects of modulus ratio, length to thickness ratio, fiber orientation, aspect ratio and various boundary conditions (SSSS, CCCC) on the critical temperature are analyzed. Argyris J. and Tenek L. 1994[4], in this study, the behavior of simply supported isotropic and thin laminated composite plates under thermal loads have examined for bending, buckling and post-buckling of symmetric angle-ply square laminates. The material properties are assumed to be independent on temperature. Finite element using triangular shell element contains 3 nodes has been implement. Sun L. and Xiaoping S. 1994[5] developed higher order displacement field for the analysis of the thermo-mechanical buckling of composite plates subjected to thermal or mechanical load. Exact closed-form solutions of symmetric cross-ply laminates are obtained using Navier method including effects of transverse shear deformation , side to thickness ratio , coefficient of thermal expansion ratio and number of layers on critical temperature and critical load. The effects played with side to thickness ratio, coefficients of thermal expansion ratio and different No. of layers. Simelane S. P. 1998 [6] studied thermal buckling of laminated composite plate using finite element computer package ABAQUS with five degrees of freedom in each node. The effect of lamination angle, modulus ratio, plate aspect ratio, and boundary constraints upon the critical buckling load temperature were investigate. Matsunaga H. 2005[7] presented higher order deformation theory for thermal buckling load of cross-ply laminated composite and sandwich square plates by using Navier method which can take into account the effects of transverse shear stress of simply supports multilayered plate. Shariyat M. 2007[8] investigated thermal buckling analysis of rectangular composite plates under uniform temperature rise based on layerwise plate theory and determine the buckling temperature using Budiansky instability criterion in a computerized solution. The effects played with boundary conditions (SSSS, CCCC) and various geometric by assuming that material property is to be varying with temperature. Rajesh et al. 2009[9] examined the random system properties on thermal buckling load of laminated composite plates under uniform temperature rise using finite

element for deriving the eigenvalue problem with and without temperature dependent elastic properties. The numerical results present that the characteristics of thermal buckling load of the plate are influence by (SSSS, CCCC and SCSC), plate thickness ratio, aspects ratio. The random system properties having random change in all input material variables, thermal expansion coefficients and plate thickness. Shiau et al. 2010[10] studied thermal buckling behavior of composite laminated plates using finite element method for cross-ply and angle-ply laminates with various degree of orthotropic, fiber angle, aspect ratio, different boundary conditions and No. of layers.

From above literature review, there are a few literatures available in thermo-mechanical field. In the present work, thermo-mechanical buckling analysis of shear deformable laminated plates with thermo-elastic properties has investigated analytically. In the present study, the temperature distribution field is assumed to be a (uniform and linear) through the plate thickness. Thermal expansion coefficients and elastic constants assumed to be independent of temperature. The formulations are based on Reddy's higher order shear deformation plate theory and classical laminated plate theory. Navier method of higher order shear deformation theory, Levy method of classical laminated plate theory and Finite element coded by ANSYS 13.0 are used to formulate the theoretical model. Many design parameters are changed to study their effects on the buckling characteristics such as No. of cross-ply and angle-ply layers, aspect ratio ( $a/b$ ), thickness ratio ( $a/h$ ), type of boundary conditions and Number of half wavelengths.

## 2. Theoretical Analysis

### 2.1 Classical Laminated Plate Theory (CLPT)

#### 2.1.1 Displacement

The displacement field of CLPT contains only three dependent variables [11]:

$$u(x,y) = u_o(x,y) + z\phi_x(x,y) \quad \dots \text{(1 a)}$$

$$v(x,y) = v_o(x,y) + z\phi_y(x,y) \quad \dots \text{(1 b)}$$

$$w(x,y) = w_o(x,y) \quad \dots \text{(1 c)}$$

Where:  $\phi_x$  ,  $\phi_y$  denote rotations about y and x axes respectively, and  $u_0$  ,  $v_0$  ,  $w_0$  denote the displacement components along (x,y,z) directions respectively of a point on the mid-plane(i.e..z=0).

### 2.1.2 Stress And Strain

The total strains can be written as follows:

$$\begin{pmatrix} \epsilon_{xx} \\ \epsilon_{yy} \\ \gamma_{xy} \end{pmatrix} = \begin{pmatrix} \epsilon_{xx}^{(0)} \\ \epsilon_{yy}^{(0)} \\ \gamma_{xy}^{(0)} \end{pmatrix} + z \begin{pmatrix} \epsilon_{xx}^{(1)} \\ \epsilon_{yy}^{(1)} \\ \gamma_{xy}^{(1)} \end{pmatrix} = \begin{pmatrix} \frac{\partial u_0}{\partial x} - \alpha_x T_0 \\ \frac{\partial v_0}{\partial y} - \alpha_y T_0 \\ \frac{\partial u_0}{\partial y} + \frac{\partial v_0}{\partial x} - \alpha_{xy} T_0 \end{pmatrix} + z \begin{pmatrix} \frac{\partial \phi_x}{\partial x} - \alpha_x T_1 \\ \frac{\partial \phi_y}{\partial y} - \alpha_y T_1 \\ \frac{\partial \phi_x}{\partial y} + \frac{\partial \phi_y}{\partial x} - \alpha_{xy} T_1 \end{pmatrix} \quad \dots (2)$$

The transformed stress-strain relations of an orthotropic lamina in a plane state of stress are; for  $\bar{Q}_{ij}$  , see [11] :

$$\begin{pmatrix} \sigma_x \\ \sigma_y \\ \sigma_{xy} \end{pmatrix}_k = \begin{bmatrix} \bar{Q}_{11} & \bar{Q}_{12} & \bar{Q}_{16} \\ \bar{Q}_{12} & \bar{Q}_{22} & \bar{Q}_{26} \\ \bar{Q}_{16} & \bar{Q}_{26} & \bar{Q}_{66} \end{bmatrix}_k \begin{pmatrix} \epsilon_{xx} - \alpha_x \Delta T \\ \epsilon_{yy} - \alpha_y \Delta T \\ \gamma_{xy} - 2\alpha_{xy} \Delta T \end{pmatrix} \quad \dots (3)$$

### 2.1.3 Equation of Motion

The Euler-Lagrange equations are obtained by setting the coefficient of  $\delta u_0$  ,  $\delta v_0$  ,  $\delta w_0$  to zero separately:

$$\delta u_0: \frac{\partial N_{xx}}{\partial x} + \frac{\partial N_{xy}}{\partial y} = 0 \quad \dots(4 a)$$

$$\delta v_0: \frac{\partial N_{xy}}{\partial x} + \frac{\partial N_{yy}}{\partial y} = 0 \quad \dots(4 b)$$

$$\delta w_0: \frac{\partial^2 M_{xx}}{\partial x^2} + 2 \frac{\partial^2 M_{xy}}{\partial x \partial y} + \frac{\partial^2 M_{yy}}{\partial y^2} + \hat{N}_{xx} \frac{\partial^2 w}{\partial x^2} + \hat{N}_{yy} \frac{\partial^2 w}{\partial y^2} = 0 \quad \dots(4 c)$$

### 2.1.4 Levy Method

Levy method, can be used to solve the governing equations of various laminated plates for which two (parallel) opposite edges are

simply supported and the other two edges can have any boundary conditions.

For cross-ply rectangular laminates with edges  $y=0$  and  $y=b$  simply supported and the other two edges  $x=\pm a/2$ , having arbitrary boundary conditions. Assume the following representation of the displacement [11]:

$$u_0(x,y,t)=\sum_{m=1}^{\infty} U_m(x) \sin\beta y \quad \dots (5 a)$$

$$v_0(x,y,t)=\sum_{m=1}^{\infty} V_m(x) \cos\beta y \quad \dots (5 b)$$

$$w_0(x,y,t)=\sum_{m=1}^{\infty} W_m(x) \sin\beta y \quad \dots (5 c)$$

Where:  $\beta = \frac{n\pi}{b}$ ;  $U_m(x)$ ,  $V_m(x)$ ,  $W_m(x)$  are independent of  $y$  (function of  $x$ )

$n$  = No. of half wavelengths in  $y$ -direction ( $n=1, 2, 3$ )

$b$  = Length of the plate along  $y$ -direction.

For angle-ply rectangular laminates with edges  $x=0$  and  $x=a$  simply supported and the other two edges  $y=\pm b/2$ , having arbitrary boundary conditions. Assume the following representation of the displacement:

$$u_0(x,y,t)=\sum_{m=1}^{\infty} U_m(y) \sin\alpha x \quad \dots (6 a)$$

$$v_0(x,y,t)=\sum_{m=1}^{\infty} V_m(y) \cos\alpha x \quad \dots (6 b)$$

$$w_0(x,y,t)=\sum_{m=1}^{\infty} W_m(y) \sin\alpha x \quad \dots (6 c)$$

Where:  $\alpha = \frac{m\pi}{a}$ ;  $a$  = Width of the plate along  $x$ -direction.

$m$  = No. of half wavelengths in  $x$ -direction ( $m= 1, 2, 3$ )

## 2.2 Third Order Shear Deformation Plate Theory (TSDT)

### 2.2.1 Displacement

The displacement field of (HSDT) is of the form [11]:

$$u(x,y,z,t)=u_0(x,y,t)+z\phi_x(x,y,t) - \frac{4}{3h^2} z^3 \left( \phi_x + \frac{\partial w_0}{\partial x} \right) \quad \dots (7 a)$$

$$v(x,y,z,t) = v_0(x,y,t) + z\phi_y(x,y,t) - \frac{4}{3h^2} z^3 \left( \phi_y + \frac{\partial w_0}{\partial y} \right) \quad \dots (7 \text{ b})$$

$$w(x,y,z,t) = w_0(x,y,t) \quad \dots (7 \text{ c})$$

### 2.2.2 Stress and Strain

The total strains can be written as follows [11] :

$$\begin{Bmatrix} \varepsilon_{xx} \\ \varepsilon_{yy} \\ \gamma_{xy} \end{Bmatrix} = \begin{Bmatrix} \varepsilon_{xx}^{(0)} \\ \varepsilon_{yy}^{(0)} \\ \gamma_{xy}^{(0)} \end{Bmatrix} + z \begin{Bmatrix} \varepsilon_{xx}^{(1)} \\ \varepsilon_{yy}^{(1)} \\ \gamma_{xy}^{(1)} \end{Bmatrix} + z^3 \begin{Bmatrix} \varepsilon_{xx}^{(3)} \\ \varepsilon_{yy}^{(3)} \\ \gamma_{xy}^{(3)} \end{Bmatrix} \quad \dots (8 \text{ a})$$

$$\begin{Bmatrix} \gamma_{yz} \\ \gamma_{xz} \end{Bmatrix} = \begin{Bmatrix} \gamma_{yz}^{(0)} \\ \gamma_{xz}^{(0)} \end{Bmatrix} + z \begin{Bmatrix} \gamma_{yz}^{(1)} \\ \gamma_{xz}^{(1)} \end{Bmatrix} + z^2 \begin{Bmatrix} \gamma_{yz}^{(2)} \\ \gamma_{xz}^{(2)} \end{Bmatrix} \quad \dots (8 \text{ b})$$

**Where:**

$$\begin{Bmatrix} \varepsilon_{xx}^{(0)} \\ \varepsilon_{yy}^{(0)} \\ \gamma_{yz}^{(0)} \\ \gamma_{xz}^{(0)} \\ \gamma_{xy}^{(0)} \end{Bmatrix} = \begin{Bmatrix} \frac{\partial u_0}{\partial x} - \alpha_x T_0 \\ \frac{\partial v_0}{\partial y} - \alpha_y T_0 \\ \frac{\partial w_0}{\partial y} + \phi_y \\ \frac{\partial w_0}{\partial x} + \phi_x \\ \frac{\partial u_0}{\partial y} + \frac{\partial v_0}{\partial x} - \alpha_{xy} T_0 \end{Bmatrix} \quad \dots (9)$$

$$\begin{Bmatrix} \varepsilon_{xx}^{(1)} \\ \varepsilon_{yy}^{(1)} \\ \gamma_{yz}^{(1)} \\ \gamma_{xz}^{(1)} \\ \gamma_{xy}^{(1)} \end{Bmatrix} = \begin{Bmatrix} \frac{\partial \phi_x}{\partial x} - \alpha_x T_1 \\ \frac{\partial \phi_y}{\partial y} - \alpha_y T_1 \\ 0 \\ 0 \\ \frac{\partial \phi_x}{\partial y} + \frac{\partial \phi_y}{\partial x} - \alpha_{xy} T_1 \end{Bmatrix} \quad \dots (10)$$

$$\begin{Bmatrix} \gamma_{yz}^{(2)} \\ \gamma_{xz}^{(2)} \end{Bmatrix} = -\frac{4}{h^2} \begin{Bmatrix} \frac{\partial w_0}{\partial y} + \phi_y \\ \frac{\partial w_0}{\partial x} + \phi_x \end{Bmatrix} \quad \dots (11)$$

$$\begin{Bmatrix} \epsilon_{xx}^{(3)} \\ \epsilon_{yy}^{(3)} \\ \gamma_{xy}^{(3)} \end{Bmatrix} = \frac{4}{3h^2} \begin{Bmatrix} \frac{\partial \phi_x}{\partial x} + \frac{\partial^2 w_0}{\partial x^2} \\ \frac{\partial \phi_y}{\partial y} + \frac{\partial^2 w_0}{\partial y^2} \\ \frac{\partial \phi_x}{\partial y} + \frac{\partial \phi_y}{\partial x} + 2 \frac{\partial^2 w_0}{\partial x \partial y} \end{Bmatrix} \quad \dots (12)$$

The transformed stress-strain relations of an orthotropic lamina in are:

$$\begin{Bmatrix} \sigma_x \\ \sigma_y \\ \sigma_{xy} \end{Bmatrix}_k = \begin{bmatrix} \bar{Q}_{11} & \bar{Q}_{12} & \bar{Q}_{16} \\ \bar{Q}_{12} & \bar{Q}_{22} & \bar{Q}_{26} \\ \bar{Q}_{16} & \bar{Q}_{26} & \bar{Q}_{66} \end{bmatrix}_k \begin{Bmatrix} \epsilon_{xx} - \alpha_x \Delta T \\ \epsilon_{yy} - \alpha_y \Delta T \\ \gamma_{xy} - 2\alpha_{xy} \Delta T \end{Bmatrix} \quad \dots (13)$$

$$\begin{Bmatrix} \sigma_{yz} \\ \sigma_{xz} \end{Bmatrix}_k = \begin{bmatrix} \bar{Q}_{44} & \bar{Q}_{45} \\ \bar{Q}_{45} & \bar{Q}_{55} \end{bmatrix} \begin{Bmatrix} \gamma_{yz} \\ \gamma_{xz} \end{Bmatrix} \quad \dots (14)$$

### 2.2.3 Equation Of Motion

The Euler-Lagrange equations are obtained by setting the coefficient of  $\delta u_0$ ,  $\delta v_0$ ,  $\delta w_0$ ,  $\delta \phi_x$ ,  $\delta \phi_y$  to zero separately [11]:

$$\delta u_0: \frac{\partial N_{xx}}{\partial x} + \frac{\partial N_{xy}}{\partial y} = 0 \quad \dots (15 a)$$

$$\delta v_0: \frac{\partial N_{xy}}{\partial x} + \frac{\partial N_{yy}}{\partial y} = 0 \quad \dots (15 b)$$

$$\delta w_0: \frac{\partial Q_x}{\partial x} - c_2 \frac{\partial R_x}{\partial x} + \frac{\partial Q_y}{\partial y} - c_2 \frac{\partial R_y}{\partial y} + c_1 \left( \frac{\partial^2 P_{xx}}{\partial x^2} + 2 \frac{\partial^2 P_{xy}}{\partial x \partial y} + \frac{\partial^2 P_{yy}}{\partial y^2} \right) + \hat{N}_{xx} \frac{\partial^2 w}{\partial x^2} + \hat{N}_{yy} \frac{\partial^2 w}{\partial y^2} + 2 \hat{N}_{xy} \frac{\partial^2 w}{\partial x \partial y} = 0 \quad \dots (15 c)$$

$$\delta \phi_x: \frac{\partial M_{xx}}{\partial x} - c_1 \frac{\partial P_{xx}}{\partial x} + \frac{\partial M_{xy}}{\partial y} - c_1 \frac{\partial P_{xy}}{\partial y} - Q_x + c_2 R_x = 0 \quad \dots (15 d)$$

$$\delta \phi_y: \frac{\partial M_{xy}}{\partial x} - c_1 \frac{\partial P_{xy}}{\partial x} + \frac{\partial M_{yy}}{\partial y} - c_1 \frac{\partial P_{yy}}{\partial y} - Q_y + c_2 R_y = 0 \quad \dots (15 e)$$

### 2.2.4 Navier Method

Navier method can be used to solve the governing equations of various laminated plates for which when all four edges of the laminate are simply supported.

For cross-ply rectangular laminates with edges  $y=0$  and  $y=b$  simply supported and the other two edges  $x=0$  and  $x=a$  simply supported. Assume the following representation of the displacement [11]:

$$u_0(x,y,t) = \sum_{n=1}^{\infty} \sum_{m=1}^{\infty} U_{mn}(t) \cos\alpha x \sin\beta y \quad \dots(16 \text{ a})$$

$$v_0(x,y,t) = \sum_{n=1}^{\infty} \sum_{m=1}^{\infty} V_{mn}(t) \sin\alpha x \cos\beta y \quad \dots(16 \text{ b})$$

$$w_0(x,y,t) = \sum_{n=1}^{\infty} \sum_{m=1}^{\infty} W_{mn}(t) \sin\alpha x \sin\beta y \quad \dots(16 \text{ c})$$

$$\phi_x(x,y,t) = \sum_{n=1}^{\infty} \sum_{m=1}^{\infty} X_{mn}(t) \cos\alpha x \sin\beta y \quad \dots(16 \text{ d})$$

$$\phi_y(x,y,t) = \sum_{n=1}^{\infty} \sum_{m=1}^{\infty} Y_{mn}(t) \sin\alpha x \cos\beta y \quad \dots(16 \text{ e})$$

Where:  $\alpha = \frac{m\pi}{a}$  ;  $\beta = \frac{n\pi}{a}$

$m$  = No. of half wavelengths in x-direction ( $m=1, 2, 3$ )

$n$  = No. of half wavelengths in y-direction ( $n=1, 2, 3$ )

$U_m$  ,  $V_m$  ,  $W_m$  are arbitrary constants to be determined;

For angle-ply rectangular laminates with edges  $y=0$  and  $y=b$  simply supported and the other two edges  $x=0$  and  $x=a$  simply supported.

Assume the following representation of the displacement [11] :

$$u_0(x,y,t) = \sum_{n=1}^{\infty} \sum_{m=1}^{\infty} U_{mn}(t) \sin\alpha x \cos\beta y \quad \dots(17 \text{ a})$$

$$v_0(x,y,t) = \sum_{n=1}^{\infty} \sum_{m=1}^{\infty} V_{mn}(t) \cos\alpha x \sin\beta y \quad \dots(17 \text{ b})$$

$$w_0(x,y,t) = \sum_{n=1}^{\infty} \sum_{m=1}^{\infty} W_{mn}(t) \sin\alpha x \sin\beta y \quad \dots(17 \text{ c})$$

$$\phi_x(x,y,t) = \sum_{n=1}^{\infty} \sum_{m=1}^{\infty} X_{mn}(t) \cos\alpha x \sin\beta y \quad \dots(17 \text{ d})$$

$$\phi_y(x,y,t) = \sum_{n=1}^{\infty} \sum_{m=1}^{\infty} Y_{mn}(t) \sin\alpha x \cos\beta y \quad \dots(17 \text{ e})$$

## 2.3 Finite Element Method

Finite element method has been employed to analyze critical buckling load for different boundary conditions and various laminate stacking sequences, aspect ratio, thickness ratio and for different number of layers. The analysis is performed to study a finite element model of the plate. The model was developed in ANSYS 13.0 using the 900 quadrature elements. The global x coordinate is directed along the width of the plate, while the global y coordinate is directed along the length and the global z direction corresponds to the thickness direction and taken to be the outward normal of the plate surface. There are 30 elements in the axial direction and 30 along the width (i.e 16926 DOF). A convergence study has been performed to select the particular mesh used in this study. A linear buckling analysis (eigenvalue buckling) was performed on the model to calculate the minimum buckling load of the structure. The finite element model is described via an input file using APDL ANSYS language with SHELL 281. SHELL 281 is suitable for analyzing thin to moderately thick shell structures. The element has eight nodes with six degrees of freedom at each node: translations in the x, y, and z axes, and rotations about the x, y, and z axes. It may be used for layered applications for modeling composite shells. It includes the effects of transverse shear deformation. The accuracy in modeling composite shells is governed by the first order shear deformation theory.

### 2.3.1 Mesh Convergence

A convergence study was performed to determine the appropriate finite element mesh to be used in the linear buckling analysis of laminated plate model. Three meshes were developed, with increasing numbers of elements in the x and y directions. The buckling load for each of these models is shown in table (1). There is only a 0.7% difference between the load calculated for mesh 1 (7\*7) and mesh 2 (15\*15). A smaller difference (0.01 %) is observed between mesh 2 and mesh 3 (30\*30). This indicates that the coarsest mesh is capable of performing the analysis within a reasonable degree of accuracy.

**Table (1): Critical Buckling Load Convergence Study for C-C-S-C Laminates**

No.of Elements	No.of Nodes	No.of DOF	Critical buckling load $N_{xx}(N/m)$
49	176	1056	10452
225	736	4416	10379
900	2821	16926	10378

### 3. Computer Programming

The main computer program has been built for Levy method and Navier method to carry out the analysis required for solving the effect of mechanical and thermal loads on buckling analysis of composite laminated plate using classical and higher order shear deformation plate theory. However they involved complex calculations that are difficult to interpret physically and require considerably more computational effort. A computer code written in MATLAB (R2010a) consisting with 1400 statements approximately. This program has the following features. See fig.(1):

1. It can solve a problem for (square, rectangular) composite laminated plate when two opposite edges are simply supported and other two edges any boundary conditions.
2. It can solve thin and thick laminated plate with any number of layers.
3. It can solve symmetric and anti-symmetric cross-ply and angle-ply composite laminated plate.
4. It can solve for critical mechanical load and critical thermal load that cause buckling and combination of these loads.

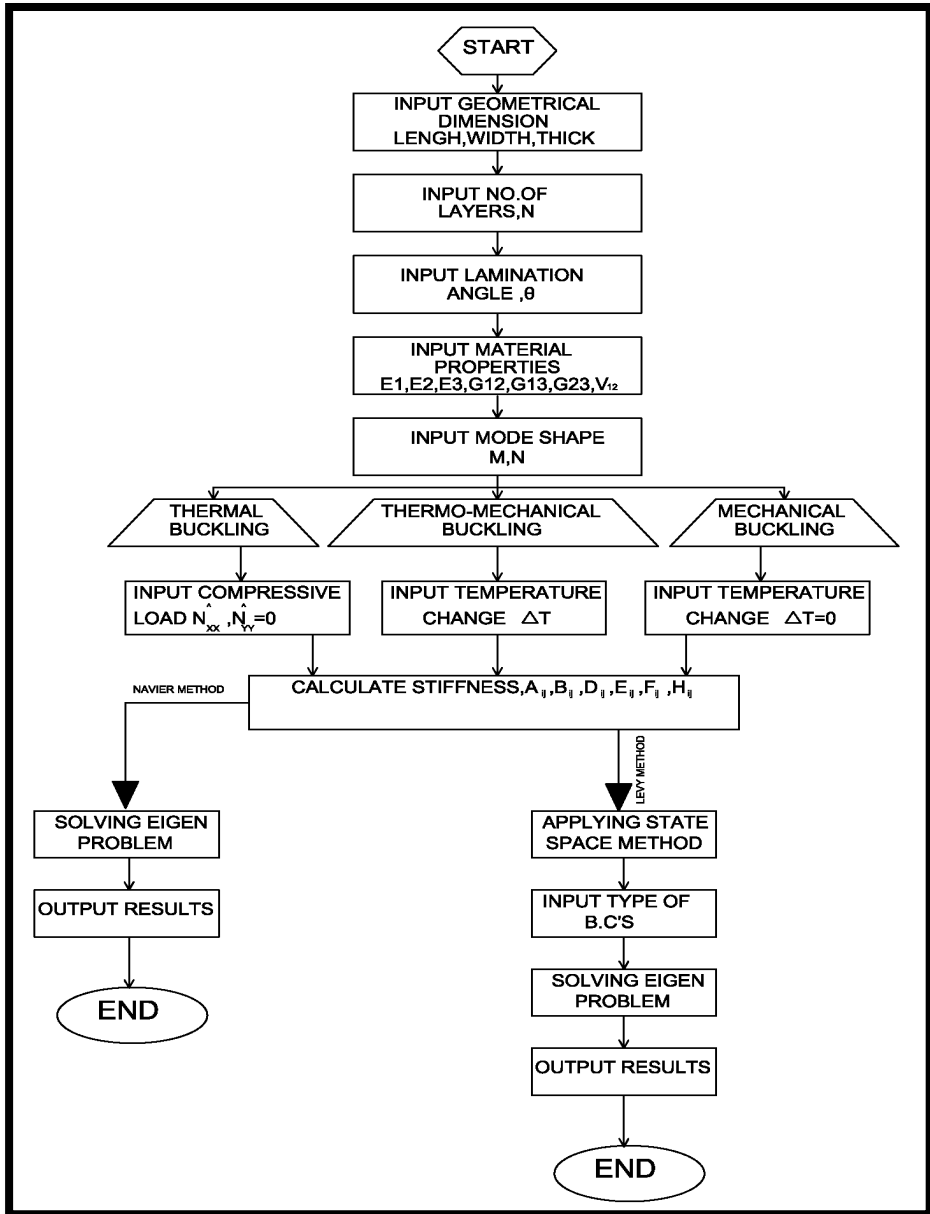
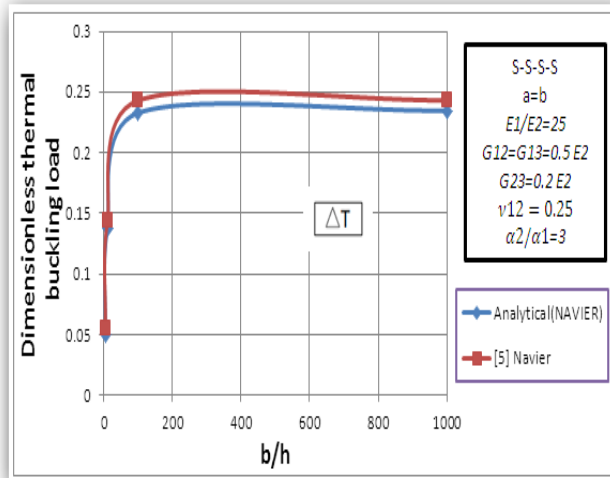


Fig. (1): MATLAB Diagram

#### 4. Verification of Computer Program

In the present study, various combinations of edge support conditions have been used for the investigation. For example,

C-S-C-S means clamped edges at  $x=0$ , a while simply supported at edges at  $y=0$  and  $b$ . To validate the present methods on the thermo-mechanical buckling analysis of different boundary conditions laminated plates, the critical buckling load (thermal , mechanical) are plotted and compared below with [5] , [9] , and [11] as shown below. The results are compared to analytical solution (Levy and Navier) and numerical solution (Finite element method), the max. Discrepancy in fig. (2) Was 4.195% when  $b/h=100$  because [5] used analytical solution (Navier method) without include membrane stiffness (that cause large deformation) while the present study include both membrane and bending stiffness.



**Fig. (2): Dimensionless Critical Temperature  $\bar{T} = T_{cr} \frac{a^2 h}{D_{22} \pi^2}$  of Symmetric Cross-Ply 0/90/90/0 Laminated Plate**

**Table (2): Dimensionless Thermal Buckling of Square Laminated Plates  $\bar{T}=T_{cr} \alpha_0 * 1000$**

b/h	laminate	B.C'S	[9] (F.E)	ANSYS 13.0 (Discrepancy %)
30	(45/-45) <sub>2T</sub>	S-S-S-S	1.133	1.131 (0.1765%)
50	(45/-45) <sub>2T</sub>	S-S-S-S	0.443	0.44101 (3.0747%)

$E2/E1=0.081$   
 $G12=G13=0.031 E1$   
 $G23=0.0304 E1$   
 $\nu12=0.21$   
 $\alpha1=-0.21 \alpha0$   
 $\alpha2=16 \alpha0$   
 $\alpha0=1e-6$

**Table. (3): Dimensionless Uniaxial Buckling Load  $\bar{N}=N_{Xx}^0 \frac{A^2}{E_2 H^3}$  of Anti-Symmetric Cross-Ply Laminates**

B.C'S	b/h	[11] Levy	Present Levy (Discrepancy %)	Present Navier (Discrepancy %)
S-F-S-F	50	16.426	17.53375 (6.3178%)	-
S-F-S-S	50	17.023	18.11575 (6.032%)	-
S-F-S-C	50	19.389	20.46825 (5.272%)	-
S-S-S-S	50	35.232	36.351 (3.078%)	-
S-S-S-C	50	59.288	60.409 (1.855%)	-
S-C-S-C	50	89.770	94.216 (4.718%)	-
S-S-S-S	5	12.109	-	13.0991 (7.558%)
S-S-S-S	10	25.423	-	24.8047 (2.432%)

$E1/E2=40$   
 $G12=G13=0.6 E2$   
 $G23=0.5 E2$   
 $\nu12=0.25$   
 $a=b$   
 $h=1$   
 $N=10$

From above results, it is obvious that the methods of solution gives better results for both thermal and mechanical loads respectively.

## 5. Experimental Analysis

### 5.1 Materials and Specimen Preparation

In the present work, the laminates which are handled lay-up include E-glass fiber/polyester laminate with fiber volume fraction approximately (0.36). Rectangular flat panels were fabricated from this material using (320 mm \* 320 mm) wood open mold with two X-ray photo sheets covered with wax matrix to avoid abrasive and insure flattening. The X-ray photo sheet were placed on the bottom of wood mold and mixed polyester (which has 0.85 g/cm<sup>3</sup> as density) and hardener together (assume each 100g polyester = 1 g hardener), and for ensuring air removal and wet out, it should cover the base surface completely especially at the end edges. The catalyzed resin was applied to the fiber layer by using brushes and rollers the fiber layer would saturate by resin. Small blade was used to take the bubble out of the fibers. The X-ray photo sheet will cover the composite and with rolling over layer to insure complete air removal. The pressure applied through the formation of the specimen is (three ceramic block) to get rid of the excess resin and remove air bubble. The panels were cured in temperature 37° C and for (3 hrs.) period of time.

The fiber volume fraction was determined from the following relationship [13]:

$$V_f = \frac{1}{1 + \frac{1-\vartheta}{\vartheta} \cdot \frac{\rho_f}{\rho_m}} \quad \dots(17 a)$$

$$\vartheta = \frac{m_f}{m_c} \quad \dots(17 b)$$

Where:

$\rho_f$  ,  $\rho_m$  : density of fiber and matrix respectively.

$m_f$  ,  $m_c$ : mass of fiber and composite respectively.

### 5.2 Tensile Test

Each laminate was oriented in longitudinal, transverse and 45° angle relative to designated 0° direction to determine the engineering parameters  $E_1$ ,  $E_2$ ,  $G_{12}$ . Test specimens were cut from the panels using water-cooled slow velocity cutting saw. Tensile test specimen includes standard geometry according to ASTM

(D638). The specimen's tensile test is mounted vertically in a servo-hydraulic testing machine, and pulled hydraulically with stroke control with large steel grips.

To determine laminate properties, recall the following definitions:

$E_1$  : Initial slope of force-elongation curve for  $0^\circ$  tensile test.

$E_2$  : Initial slope of force-elongation curve for  $90^\circ$  tensile test.

$E_x$  : Initial slope of force-elongation curve for  $(\pm 45^\circ)$  tensile test.

The shear modulus  $G_{12}$  is determined from following equation:

$$\frac{1}{E_x} = \frac{\cos^4\theta}{E_1} + \frac{\sin^4\theta}{E_2} + \left( \frac{1}{G_{12}} - \frac{2\nu_{21}}{E_2} \right) \sin^2\theta \cos^2\theta \quad \dots (18)$$

## 6. Results and Discussions Theoretical Analysis

The present study focused mainly on the buckling behavior of composite laminated plates subjected to thermal (uniform, linear) and thermo-mechanical loads are analyzed by analytical analysis and numerical analysis for different aspect ratio, thickness ratio, lamination angle and No. of layers with various boundary conditions. In present work, mechanical properties for glass-polyester are obtained from experimental results as shown in table (4).

**Table. (4): Experimental Mechanical Properties of Fiber Glass-Polyester**

Mechanical properties	Glass-polyester
$E_1$ (GPa)	6.981
$E_2 = E_3$ (GPa)	2.0566
$G_{12} = G_{13}$	0.8979
$G_{13} = G_{23}$ (GPa)(assume)	0.8979
$\nu_{12}$ [5]	0.28
$\alpha_{xx}$ ( $1/C^\circ$ ) [12]	$8.6 \alpha_0$
$\alpha_{yy}$ ( $1/C^\circ$ ) [12]	$22.1 \alpha_0$
$\alpha_0$ ( $1/C^\circ$ )	$10^{-6}$
$V_f$	0.36

### 6.1 Laminated Plate Subjected to Thermal Load

In table (5) (Temperature varying uniformly) and fig. (3) (Temperature varying linearly), it can be obtained that the buckling load is decrease with high percentage when a/b varies from 0.5 to 1. On other hand, this percentage get smaller when a/b varies from 1 to 2

**Table. (5): Dimensionless Linear Thermal buckling load [  $\bar{T} = T_{cr} * \alpha_0 * 1000$  ] versus aspect ratio , (a/b) of an anti-symmetric cross-ply ( 0/90/0/90 )<sub>S</sub> laminates**

a/b	F-S-S-S	F-S-F-S
0.5	0.02648	0.01357
1	0.01581	0.0133
1.5	0.014	0.013
2	0.0132	0.01287

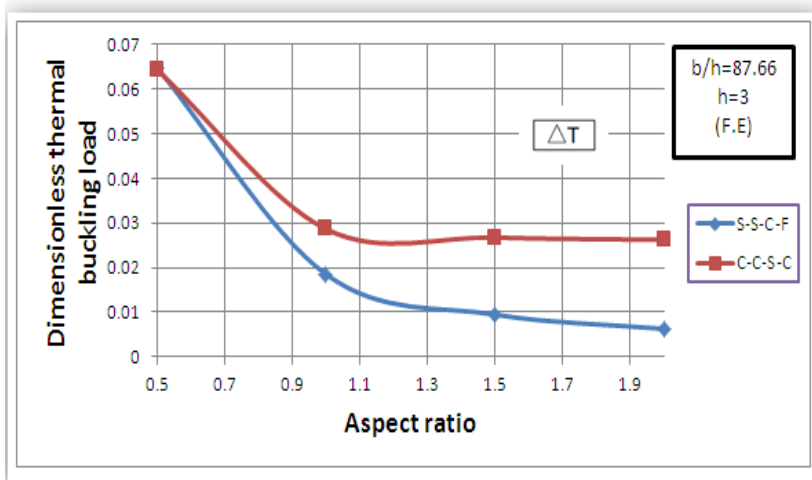


**Fig. (3): Dimensionless Uniform Thermal Buckling Load [  $\bar{T} = T_{cr} * \alpha_0 * 1000$  ] Versus Aspect Ratio , (A/B) of An Anti-Symmetric Cross-Ply ( 0/90/0/90 )<sub>T</sub> Laminates**

Fig.(4 a) shows the deformation shape of laminated plate at mode1 where the min. load that cause buckling (critical load) occurs in the first mode shape, while fig.(4 b) gives an overall evaluation of deflection state on laminated plate for the first mode shape too .

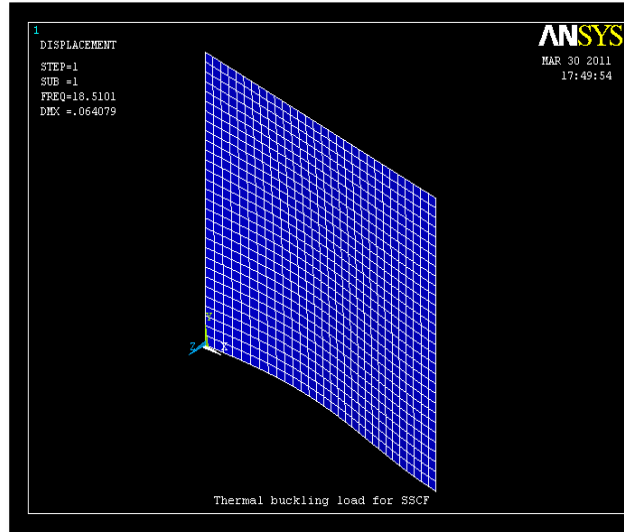


**Fig. (4 A): Deformed Shape of Laminated Plate for Mode 1**

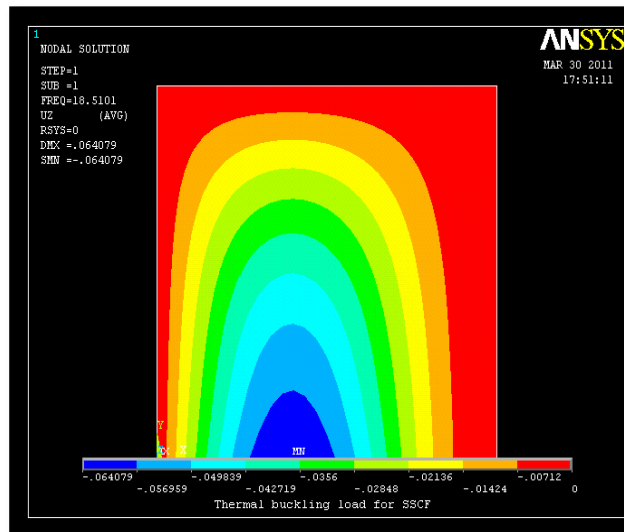


**Fig. (4 B): Deflection of Laminated Plate for Mode 1**

From Fig. (5)(Temperature varying uniformly), it is clear to noted that the buckling load increase with small percentage in cases S-C-S-F and S-S-S-F when  $\theta$  varies from 10 to 30 because of the effect of B.C'S to be more constraint. The increase in buckling load in S-C-S-F is more than in S-S-S-F where this increase reaches to 6.0427%. Then, the buckling load decrease when  $\theta$  varies from 30 to 80. The decrease in buckling load is S-S-S-F is more than S-C-S-F where this decrease reaches to 40.486%. On other hand, the buckling load in S-F-S-F decrease with high percentage when  $\theta$  varies from 10 to 80. This decrease reaches to 58.469%.

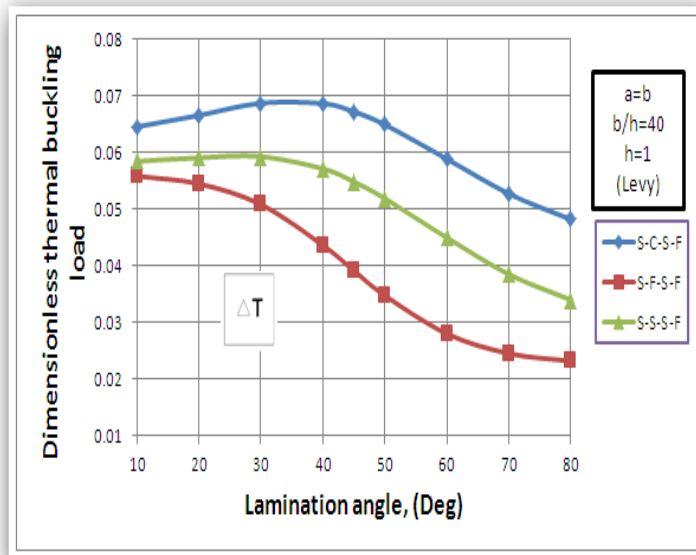


**Fig. (5): Dimensionless Uniform Thermal Buckling Load [  $\bar{T} = T_{cr} * \alpha_0 * 1000$  ] Versus Lamination Angle , ( $\theta$ ) of An Anti-Symmetric Angle-Ply (  $\theta / -\theta / \theta / -\theta$  ) Laminates**

## 6.2 Laminated Plate Subjected to Thermo-Mechanical Load

In table (6) and (7), the uniaxial buckling load for different cases is summarized. It is important to note that the max. Buckling load decreases with different percentage when  $T$  increases. It is evident that the decrease in buckling load in table (6) deals with thin

laminated plate for different B.C'S. The decrease in buckling load for case S-S-S-S is more than other cases because of the effect of B.C'S, this decrease reaches to 85%, while the decrease in buckling load in C-S-C-S is less than other cases where this decrease reaches to 25.33%.

**Table. (6): Dimensionless Uniaxial Buckling Load**  
 $[\bar{N} = N_{yy}^0 * b^2 / E_2 * h^3]$  **of Laminated Plates Under Uniformly**  
**Temperature Distribution**

Lamination Scheme	Boundary condition	a/b	Thick. Ratio a/h	Buckling load (Levy)			
				$\Delta T=0^\circ C$	$\Delta T=10^\circ C$	$\Delta T=20^\circ C$	$\Delta T=30^\circ C$
$(0/90/0/90)_T$	S-S-S-S	0.5	43.833	22.5 <sub>2</sub>	17.787 <sub>2</sub>	13.0738 <sub>2</sub>	3.3733
$(0/90/0/90)_T$	C-S-C-S	0.5	43.833	43.1 <sub>3</sub>	39.455 <sub>3</sub>	35.821 <sub>3</sub>	32.181 <sub>3</sub>
$(0/90/0/90)_T$	C-S-S-S	0.5	43.833	33.7 <sub>3</sub>	29.138 <sub>2</sub>	24.058 <sub>2</sub>	18.9655 <sub>2</sub>

**Table. (7): Dimensionless Uniaxial Buckling Load**  
 $[\bar{N} = N_{yy}^0 * b^2 / E_2 * h^3]$  **of Laminated Plates Under Uniformly**  
**Temperature Distribution**

Lamination Scheme	Boundary condition	a/b	b/h	Buckling load (Navier)			
				$\Delta T=0^\circ C$	$\Delta T=20^\circ C$	$\Delta T=40^\circ C$	$\Delta T=60^\circ C$
$(0/90/0)_T$	S-S-S-S	1	10	4.9649	4.786	4.6659	4.5457
$(0/90/0)_T$	S-S-S-S	1	20	5.2669	4.7204	4.2398	3.7592
$(0/90/0)_S$	S-S-S-S	1	10	5.0268	4.8471	4.727	4.6068
$(0/90/0)_S$	S-S-S-S	1	20	5.3425	4.7951	4.3145	3.8339
$(50/-50/50)_T$	S-S-S-S	1	10	6.3893	6.2397	6.1196	5.9994
$(50/-50/50)_T$	S-S-S-S	1	20	6.889	6.3741	5.8935	5.413
$(0/90)_S$	S-S-S-S	1.5	10	2.2892	2.1757	2.0889	2.0022
$(0/90/90/0/0)_S$	S-S-S-S	1.5	10	2.75	2.6356	2.55	2.4645
$(0/90)_T$	S-S-S-S	1.5	10	2.702	2.5887	2.5019	2.4151
$(0/90/90/0/0)_T$	S-S-S-S	1.5	10	2.5406	2.455	2.3694	2.2838
$(45/-45/45/-45/45)_T$	S-S-S-S	1.5	10	3.3701	3.2833	3.1966	3.1098

On other hand, the decrease in buckling load in table (7) for  $(0/90/0)_T$ ,  $(b/h=20)$  is more than other cases, this decrease reaches 28.62% , while this percentage in  $(50/-50/50)_T$ ,  $(b/h=10)$  become less than other cases, it reaches to 6.1%.

In fig.(6), it is evident that the uniaxial buckling load decrease with temperature increasing, the decrease in buckling load gets higher when T varies from 40°C to 60°C. The percentage of this decrease reaches to 1.19%. On other hand, the decrease in buckling load gets lower when T varies from 20°C to 40°C. The percentage of this decrease reaches to 1.1%.

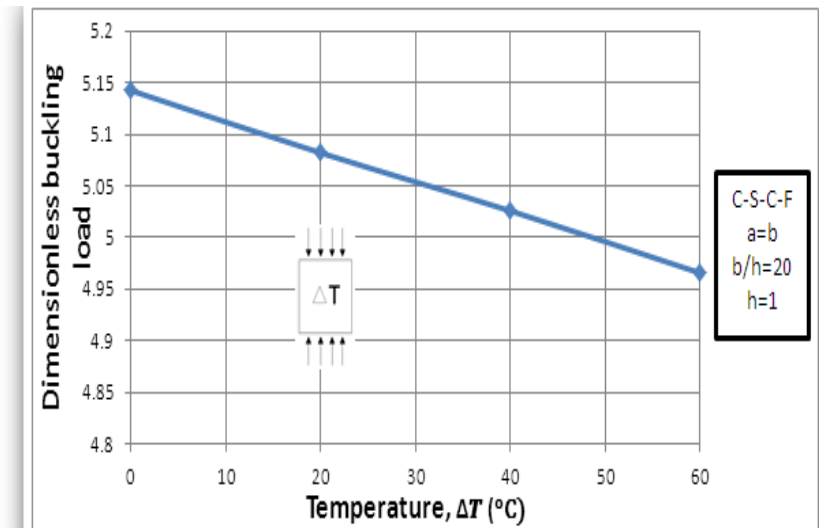


**Fig. (6): Dimensionless Uniaxial Buckling Load**  
 $[\bar{N} = N_{yy}^0 * b^2 / E_2 * h^3]$  **Versus Uniformly Temperature**  
**Distribution of An Anti-Symmetric Cross-Ply  $(0/90/0/90)_T$**   
**Laminates**

## 7. Conclusion

This study considers the buckling analysis of cross-ply and angle-ply laminates with various B.C's. From the present analytical study, the following conclusions can be made:

1. It was noted that different thickness ratio affected the critical buckling load. The buckling load decrease when side to

thickness ratio ( $b/h$ ) increases because the effects of boundary on the middle region of the laminated plate diminish. so that, the buckling load encounters a significant decrease.

2. As the aspect ratio increases, the critical buckling load of laminated plate decreases and reaches to min. value at  $a/b=2$  because the boundary effects on the middle region of the laminated plate decreases and consequently, the buckling load decreases. The max. decrease in buckling load occurs when  $a/b$  varies from 0.5 to 1.
3. It was seen that the different fiber orientation angles affected the critical buckling load. When the fiber angle increases, the buckling load increases with small percentage in case S-C-S-F and S-S-S-F when  $\theta$  varies from 10 to 30. Then, the buckling load decreases. On other hand, the buckling load in S-F-S-F decreases with high percentage when  $\theta$  varies from 10 to 80 and reaches to min. value at  $\theta=80$ .
4. It is clear that No. of layers affected on critical buckling load. The buckling load increase asymptotically when No. of layers increase.
5. The boundary conditions affect the buckling load, the buckling load increase when boundary conditions become more stiffness.

## References

- [1] Gossard M.L., Seide P., and Roberts W.M. "Thermal buckling of plates ". NASA TN 2771; 1952.
- [2] Thangaratnam K.R., Palaninathan, and Ramachandran J. "Thermal buckling of composite laminated plates ". J computers and structures 1988; 32(5): 1117-1124.
- [3] Prabhu M.R. and Dhanaraj R. "Thermal buckling of laminated composite plates ". J computers and structures 1994; 53(5): 1193-1204.
- [4] Argyris J. and Tenek L. "High-temperature bending, buckling and postbuckling of laminated composite plates using the natural

- mode method “. J computer methods in applied mechanics and engineering 1994; 117:105-142.
- [5] Sun L. and Xiaoping S. “Thermo-mechanical buckling of laminated composite plates with higher-order transverse shear deformation “. J computers and structures 1994; 53(1): 1-7.
- [6] Simelane S. P. “ Thermal buckling of laminated composite Plates”. M.Sc. thesis; South Africa; 1998.
- [7] Matsunaga H. “Thermal buckling of cross-ply laminated composite and sandwich plates according to a global higher-order deformation theory “. J composite structures 2005; 68:439-454.
- [8] Shariyat M. “Thermal buckling analysis of rectangular composite plates with temperature-dependent properties based on a layerwise theory “. J thin-walled structures 2007; 45:439-452.
- [9] Rajesh K., Lal A., and Singh B.N. “Effects of random system properties on the thermal buckling analysis of laminated composite plated “. J computers and structures 2009; 87:1119-1128..
- [10] Shiau L., Kuo S., and Chen C. “Thermal buckling behavior of composite laminated plates “. J composite structures 2010; 92: 508-514.
- [11] Reddy J.N. “Mechanics of laminated composite plates and shells: theory and analysis “. 2ed; CRC Press 2004.
- [12] Zaffer G. “Design and optimization of laminated composite materials “. Canada; John Wiley & Sons 1999.
- [13] United States of America ; Department of Defense “ Composite Material Handbook” vol 2; 2002.

## Appendix A

### Classical laminated plate theory

The in-plane force resultants are defined as

$$\begin{Bmatrix} N_{xx} \\ N_{yy} \\ N_{xy} \end{Bmatrix} = \int_{-h/2}^{h/2} \begin{Bmatrix} \sigma_x \\ \sigma_y \\ \sigma_{xy} \end{Bmatrix}_k dz = \sum_{r=1}^N \int_{z_k}^{z_{k+1}} \begin{Bmatrix} \sigma_x \\ \sigma_y \\ \sigma_{xy} \end{Bmatrix}_k dz \quad \dots (A-1)$$

Where  $\sigma_x$ ,  $\sigma_y$  and  $\tau_{xy}$  are normal and shear stress.

$\alpha_x$ ,  $\alpha_y$  and  $\alpha_{xy}$  are thermal expansion coefficients

$$\begin{Bmatrix} N_{xx} \\ N_{yy} \\ N_{xy} \end{Bmatrix} = \begin{bmatrix} A_{11} & A_{12} & A_{16} \\ A_{12} & A_{22} & A_{26} \\ A_{16} & A_{26} & A_{66} \end{bmatrix} \begin{Bmatrix} \varepsilon_{xy}^0 \\ \varepsilon_{xy}^0 \\ \gamma_{xy}^0 \end{Bmatrix} + \begin{bmatrix} B_{11} & B_{12} & B_{16} \\ B_{12} & B_{22} & B_{26} \\ B_{16} & B_{26} & B_{66} \end{bmatrix} \begin{Bmatrix} \varepsilon_{xx}^1 \\ \varepsilon_{yy}^1 \\ \gamma_{xy}^1 \end{Bmatrix} - \begin{Bmatrix} N_x^T \\ N_y^T \\ N_{xy}^T \end{Bmatrix} \dots (A-2)$$

$$\begin{Bmatrix} M_{xx} \\ M_{yy} \\ M_{xy} \end{Bmatrix} = \int_{-h/2}^{h/2} \begin{Bmatrix} \sigma_x \\ \sigma_y \\ \sigma_{xy} \end{Bmatrix}_k z dz = \sum_{r=1}^N \int_{z_k}^{z_{k+1}} \begin{Bmatrix} \sigma_x \\ \sigma_y \\ \sigma_{xy} \end{Bmatrix}_k z dz \quad \dots (A-3)$$

$$\begin{Bmatrix} M_{xx} \\ M_{yy} \\ M_{xy} \end{Bmatrix} = \begin{bmatrix} B_{11} & B_{12} & B_{16} \\ B_{12} & B_{22} & B_{26} \\ B_{16} & B_{26} & B_{66} \end{bmatrix} \begin{Bmatrix} \varepsilon_{xy}^0 \\ \varepsilon_{xy}^0 \\ \gamma_{xy}^0 \end{Bmatrix} + \begin{bmatrix} D_{11} & D_{12} & D_{16} \\ D_{12} & D_{22} & D_{26} \\ D_{16} & D_{26} & D_{66} \end{bmatrix} \begin{Bmatrix} \varepsilon_{xx}^1 \\ \varepsilon_{yy}^1 \\ \gamma_{xy}^1 \end{Bmatrix} - \begin{Bmatrix} M_x^T \\ M_y^T \\ M_{xy}^T \end{Bmatrix} \dots (A-4)$$

Where  $\{N^T\}$  and  $\{M^T\}$  are thermal stress and bending results, respectively

$$\begin{Bmatrix} N_x^T, M_x^T \\ N_y^T, M_y^T \\ N_{xy}^T, M_{xy}^T \end{Bmatrix} = \sum_{k=1}^N \int_{-h/2}^{h/2} \begin{bmatrix} \bar{Q}_{11} & \bar{Q}_{12} & \bar{Q}_{16} \\ \bar{Q}_{12} & \bar{Q}_{22} & \bar{Q}_{26} \\ \bar{Q}_{16} & \bar{Q}_{26} & \bar{Q}_{66} \end{bmatrix} \begin{Bmatrix} \alpha_x \\ \alpha_y \\ 2\alpha_{xy} \end{Bmatrix} (1, z) \Delta T dz \quad \dots (A-5)$$

For uniform temperature variation:

$$\Delta T = \text{applied temperature} - \text{reference temperature} \quad \dots \text{ (A-6)}$$

For linear temperature variation:

$$\Delta T = T_0(x,y,t) + z * T_1(x,y,t) \quad \dots \text{ (A-7)}$$

Here,  $A_{ij}$  are the extensional stiffness,  $B_{ij}$  the coupling stiffness, and  $D_{ij}$  the bending stiffness.

$$A_{ij} = \sum_{k=1}^N (\bar{Q}_{ij})_k (z_{k+1} - z_k) \quad \dots \text{ (A-8)}$$

$$B_{ij} = \frac{1}{2} \sum_{k=1}^N (\bar{Q}_{ij})_k (z_{k+1}^2 - z_k^2) \quad \dots \text{ (A-9)}$$

$$D_{ij} = \frac{1}{3} \sum_{k=1}^N (\bar{Q}_{ij})_k (z_{k+1}^3 - z_k^3) \quad \dots \text{ (A-10)}$$

**APPENDIX B**

Third order shear deformation plate theory

The in-plane force resultants are defined as:

$$\begin{Bmatrix} N_{xx} \\ N_{yy} \\ N_{xy} \end{Bmatrix} = \int_{-h/2}^{h/2} \begin{Bmatrix} \sigma_x \\ \sigma_y \\ \sigma_{xy} \end{Bmatrix}_k dz = \sum_{r=1}^N \int_{z_k}^{z_{k+1}} \begin{Bmatrix} \sigma_x \\ \sigma_y \\ \sigma_{xy} \end{Bmatrix}_k dz \quad \dots \text{(B-1)}$$

$$\begin{Bmatrix} N_{xx} \\ N_{yy} \\ N_{xy} \end{Bmatrix} = \begin{bmatrix} A_{11} & A_{12} & A_{16} \\ A_{12} & A_{22} & A_{26} \\ A_{16} & A_{26} & A_{66} \end{bmatrix} \begin{Bmatrix} \varepsilon_{xy}^0 \\ \varepsilon_{xy}^0 \\ \gamma_{xy}^0 \end{Bmatrix} + \begin{bmatrix} B_{11} & B_{12} & B_{16} \\ B_{12} & B_{22} & B_{26} \\ B_{16} & B_{26} & B_{66} \end{bmatrix} \begin{Bmatrix} \varepsilon_{xx}^1 \\ \varepsilon_{yy}^1 \\ \gamma_{xy}^1 \end{Bmatrix} -$$

$$c_1 \begin{bmatrix} E_{11} & E_{12} & E_{16} \\ E_{12} & E_{22} & E_{26} \\ E_{16} & E_{26} & E_{66} \end{bmatrix} \begin{Bmatrix} \varepsilon_{xx}^{(3)} \\ \varepsilon_{yy}^{(3)} \\ \gamma_{xy}^{(3)} \end{Bmatrix} - \begin{Bmatrix} N_x^T \\ N_y^T \\ N_{xy}^T \end{Bmatrix} \quad \dots \text{(B-2)}$$

$$\begin{Bmatrix} M_{xx} \\ M_{yy} \\ M_{xy} \end{Bmatrix} = \int_{-h/2}^{h/2} \begin{Bmatrix} \sigma_x \\ \sigma_y \\ \sigma_{xy} \end{Bmatrix}_k z dz = \sum_{r=1}^N \int_{z_k}^{z_{k+1}} \begin{Bmatrix} \sigma_x \\ \sigma_y \\ \sigma_{xy} \end{Bmatrix}_k z dz \quad \dots \text{(B-3)}$$

$$\begin{Bmatrix} M_{xx} \\ M_{yy} \\ M_{xy} \end{Bmatrix} = \begin{bmatrix} B_{11} & B_{12} & B_{16} \\ B_{12} & B_{22} & B_{26} \\ B_{16} & B_{26} & B_{66} \end{bmatrix} \begin{Bmatrix} \varepsilon_{xy}^0 \\ \varepsilon_{xy}^0 \\ \gamma_{xy}^0 \end{Bmatrix} + \begin{bmatrix} D_{11} & D_{12} & D_{16} \\ D_{12} & D_{22} & D_{26} \\ D_{16} & D_{26} & D_{66} \end{bmatrix} \begin{Bmatrix} \varepsilon_{xx}^1 \\ \varepsilon_{yy}^1 \\ \gamma_{xy}^1 \end{Bmatrix} -$$

$$c_1 \begin{bmatrix} F_{11} & F_{12} & F_{16} \\ F_{12} & F_{22} & F_{26} \\ F_{16} & F_{26} & F_{66} \end{bmatrix} \begin{Bmatrix} \varepsilon_{xx}^{(3)} \\ \varepsilon_{yy}^{(3)} \\ \gamma_{xy}^{(3)} \end{Bmatrix} - \begin{Bmatrix} M_x^T \\ M_y^T \\ M_{xy}^T \end{Bmatrix} \quad \dots \text{(B-4)}$$

$$\begin{Bmatrix} P_{xx} \\ P_{yy} \\ P_{xy} \end{Bmatrix} = \int_{-h/2}^{h/2} \begin{Bmatrix} \sigma_x \\ \sigma_y \\ \sigma_{xy} \end{Bmatrix}_k z^3 dz = \sum_{k=1}^N \int_{z_k}^{z_{k+1}} \begin{Bmatrix} \sigma_x \\ \sigma_y \\ \sigma_{xy} \end{Bmatrix}_k z^3 dz \quad \dots \text{(B-5)}$$

$$\begin{Bmatrix} P_{xx} \\ P_{yy} \\ P_{xy} \end{Bmatrix} = \begin{bmatrix} E_{11} & E_{12} & E_{16} \\ E_{12} & E_{22} & E_{26} \\ E_{16} & E_{26} & E_{66} \end{bmatrix} \begin{Bmatrix} \varepsilon_{xy}^0 \\ \varepsilon_{xy}^0 \\ \gamma_{xy}^0 \end{Bmatrix} + \begin{bmatrix} F_{11} & F_{12} & F_{16} \\ F_{12} & F_{22} & F_{26} \\ F_{16} & F_{26} & F_{66} \end{bmatrix} \begin{Bmatrix} \varepsilon_{xx}^1 \\ \varepsilon_{yy}^1 \\ \gamma_{xy}^1 \end{Bmatrix} - c_1 \begin{bmatrix} H_{11} & H_{12} & H_{16} \\ H_{12} & H_{22} & H_{26} \\ H_{16} & H_{26} & H_{66} \end{bmatrix} \begin{Bmatrix} \varepsilon_{xx}^{(3)} \\ \varepsilon_{yy}^{(3)} \\ \gamma_{xy}^{(3)} \end{Bmatrix} - \begin{Bmatrix} P_x^T \\ P_y^T \\ P_{xy}^T \end{Bmatrix} \dots \text{(B-6)}$$

$$\begin{Bmatrix} Q_{yz} \\ Q_{xz} \end{Bmatrix} = \int_{-h/2}^{h/2} \begin{Bmatrix} \sigma_{yz} \\ \sigma_{xz} \end{Bmatrix}_k dz = \sum_{k=1}^N \int_{z_k}^{z_{k+1}} \begin{Bmatrix} \sigma_{yz} \\ \sigma_{xz} \end{Bmatrix}_k dz \dots \text{(B-7)}$$

$$\begin{Bmatrix} Q_{yz} \\ Q_{xz} \end{Bmatrix} = \begin{bmatrix} A_{44} & A_{45} \\ A_{45} & A_{55} \end{bmatrix} \begin{Bmatrix} \gamma_{yz}^{(0)} \\ \gamma_{xz}^{(0)} \end{Bmatrix} - c_2 \begin{bmatrix} D_{44} & D_{45} \\ D_{45} & D_{55} \end{bmatrix} \begin{Bmatrix} \gamma_{yz}^{(2)} \\ \gamma_{xz}^{(2)} \end{Bmatrix} \dots \text{(B-8)}$$

$$\begin{Bmatrix} R_{yz} \\ R_{xz} \end{Bmatrix} = \int_{-h/2}^{h/2} \begin{Bmatrix} \sigma_{yz} \\ \sigma_{xz} \end{Bmatrix}_k z^2 dz = \sum_{k=1}^N \int_{z_k}^{z_{k+1}} \begin{Bmatrix} \tau_{yz} \\ \tau_{xz} \end{Bmatrix}_k z^2 dz \dots \text{(B-9)}$$

$$\begin{Bmatrix} R_{yz} \\ R_{xz} \end{Bmatrix} = \begin{bmatrix} D_{44} & D_{45} \\ D_{45} & D_{55} \end{bmatrix} \begin{Bmatrix} \gamma_{yz}^{(0)} \\ \gamma_{xz}^{(0)} \end{Bmatrix} - c_2 \begin{bmatrix} F_{44} & F_{45} \\ F_{45} & F_{55} \end{bmatrix} \begin{Bmatrix} \gamma_{yz}^{(2)} \\ \gamma_{xz}^{(2)} \end{Bmatrix} \dots \text{(B-10)}$$

Where

$$A_{ij}, B_{ij}, D_{ij}, E_{ij}, F_{ij}, H_{ij} = \sum_{k=1}^N \int_{z_k}^{z_{k+1}} \bar{Q}_{ij}^{(k)} (1, z, z^2, z^3, z^4, z^6) dz \dots \text{(B-11)}$$

Where  $\{N^T\}, \{M^T\}$  and  $\{P^T\}$  are thermal stress results

$$\begin{Bmatrix} N_x^T, M_x^T, P_x^T \\ N_y^T, M_y^T, P_y^T \\ N_{xy}^T, M_{xy}^T, P_{xy}^T \end{Bmatrix} = \sum_{k=1}^N \int_{-h/2}^{h/2} \begin{bmatrix} \bar{Q}_{11} & \bar{Q}_{12} & \bar{Q}_{16} \\ \bar{Q}_{12} & \bar{Q}_{22} & \bar{Q}_{26} \\ \bar{Q}_{16} & \bar{Q}_{26} & \bar{Q}_{66} \end{bmatrix} \begin{Bmatrix} \alpha_x \\ \alpha_y \\ 2\alpha_{xy} \end{Bmatrix} (1, z, z^3) \Delta T dz \dots \text{(B-12)}$$

## Nomenclature

Symbol	Description	Unit
a	Dimension along x-coordinate	m
b	Dimension along y-coordinate	m
$A_{ij}$ , $B_{ij}$ , $D_{ij}$ , $E_{ij}$ , $F_{ij}$ , $H_{ij}$	Extensional, bending extensional coupling, bending and additional stiffness	-
$E_1$ , $E_2$ , $E_3$	Elastic modulus components	Gpa
$G_{12}$ , $G_{23}$ , $G_{13}$	Shear modulus components	Gpa
h	Thickness	m
m, n	No. of half wavelengths in x and y directions	-
N	Total number of plate layers	-
$N_{xx}$ , $N_{yy}$ , $N_{xy}$	In-plane force resultant	N/m
$M_{xx}$ , $M_{yy}$ , $M_{xy}$	Moment resultant per unit length	N.m/m
$P_{xx}$ , $P_{yy}$ , $P_{xy}$	Resultant force per unit length	N/m
$Q_{xz}$ , $Q_{yz}$	Transverse shear force resultant	N
$R_{xz}$ , $R_{yz}$	Transverse shear force resultant (HSDT)	N

Symbol	Description	Unit
$\bar{Q}_{ij}^{(k)}$	Transformed lamina stiffness	N/m
$z$	Distance from neutral axis	m
$x, y, z$	Cartesian coordinate system	m
$Z_k, Z_{k+1}$	Upper and lower lamina surface coordinates along z-direction	m
$\alpha_{xx}, \alpha_{yy}, \alpha_{xy}$	Transformed thermal coefficients of expansion	$1/C^0$
$\epsilon_{xx}, \epsilon_{yy}, \epsilon_{xy}, \epsilon_{xz}, \epsilon_{yz}, \epsilon_{zz}$	Strain components	m/m
$\Delta T$	Temperature increment	$C^0$
$\gamma_{xz}, \gamma_{yz}$	Transverse shear strain	m/m
$\nu_{12}$	Poisson's ratio component	-
$\sigma_{xx}, \sigma_{yy}, \sigma_{xy}, \sigma_{xz}, \sigma_{yz}$	Stress components	Gpa
C-S-C-S	Clamped at x-axis and simply supported at y-axis	-
$N_{xx}^T, N_{yy}^T$	Thermal stress resultant	N/m
$N_{xx}^0, N_{yy}^0$	Applied edge forces	N/m
$\theta$	Fiber orientation angle	Degree
$U_{mn}, V_{mn}, W_{mn}, X_{mn}, Y_{mn}$	Arbitrary constant	-

Symbol	Description	Unit
T	Temperature	$C^{\circ}$
1, 2, 3	Principal material coordinate system	-
$(0/90)_S$	Symmetric cross-ply laminate	-
$(0/90)_T$	Anti-symmetric cross-ply laminate	-
$(\theta/-\theta)_T$	Anti-symmetric angle-ply laminate	-
$(\theta/-\theta)_S$	Symmetric angle-ply laminate	-
S	Simply supported edge	-
C	Clamped edge	-
F	Free edge	-
$\rho_f$	Density of fiber	-
$\rho_m$	Density of matrix	-
mf	Mass of fiber	-
mc	Mass of composite	-

## تحليل الانبعاج للصفائح المركبة تحت تأثير الأحمال الحرارية والميكانيكية

أ.د. عدنان ناجي جميل      م.م. حسنين ابراهيم نصيف

جامعة بغداد – كلية الهندسة  
قسم الهندسة الميكانيكية

### المستخلص:

يتضمن البحث دراسة وتحليل الانبعاج لصفائح المواد المركبة المعرضة للاحمال الحرارية (المنتظمة والخطية) والميكانيكية نظريا. في الجانب النظري تم دراسة معادلات الحركة عن النظرية الكلاسيكية CLPT وعن نظرية اجهاد القص ذات الرتبة العالية HSDT وتم اشتقاق هذه المعادلات وحلها تحليليا باستخدام طريقة نافير وطريقة ليفي لجميع انواع الاسناد للصفائح المركبة المتماثلة وغير المتماثلة مع الاخذ بنظر الاعتبار تأثير ال mode shape ،نسبة طول الى عرض الصفيحة ، عدد الطبقات ، زاوية دوران الياف الطبقات ، ونسبة نحافة الطبقات وتأثيرها على الحمل الحرج المسبب في تأثير الانبعاج بحل مسألة Eigen value للاحمال الحرارية والميكانيكية ، وايضا تم تحليل حمل الانبعاج الحرج عدديا باستخدام طريقة العناصر المحددة. يتضمن الجانب العملي حساب الخواص الميكانيكية (ضمن درجة حرارة الغرفة) لمادة الفايبر كلاس – بوليستر. النتائج التي تم الحصول عليها اعطت موافقة جيدة مع النتائج المنشورة لباحثين اخرين.